

Supporting information for:

**Cross-coupling polymerization at iodophenyl thin films prepared by spontaneous grafting of a diazonium salt**

Nicholas Marshall<sup>1</sup> and Andres Rodriguez<sup>2</sup>

1. University of South Carolina Aiken, Department of Chemistry and Physics.

2. College of Pharmacy, Medical University of South Carolina, 280 Calhoun Street, Charleston, SC 29425, USA

471 University Parkway, Aiken, SC, 29801, USA. Tel: 1.803.641.3409; E-mail:  
nicholasm@usca.edu.<http://orcid.org/0000-0001-8048-0857>

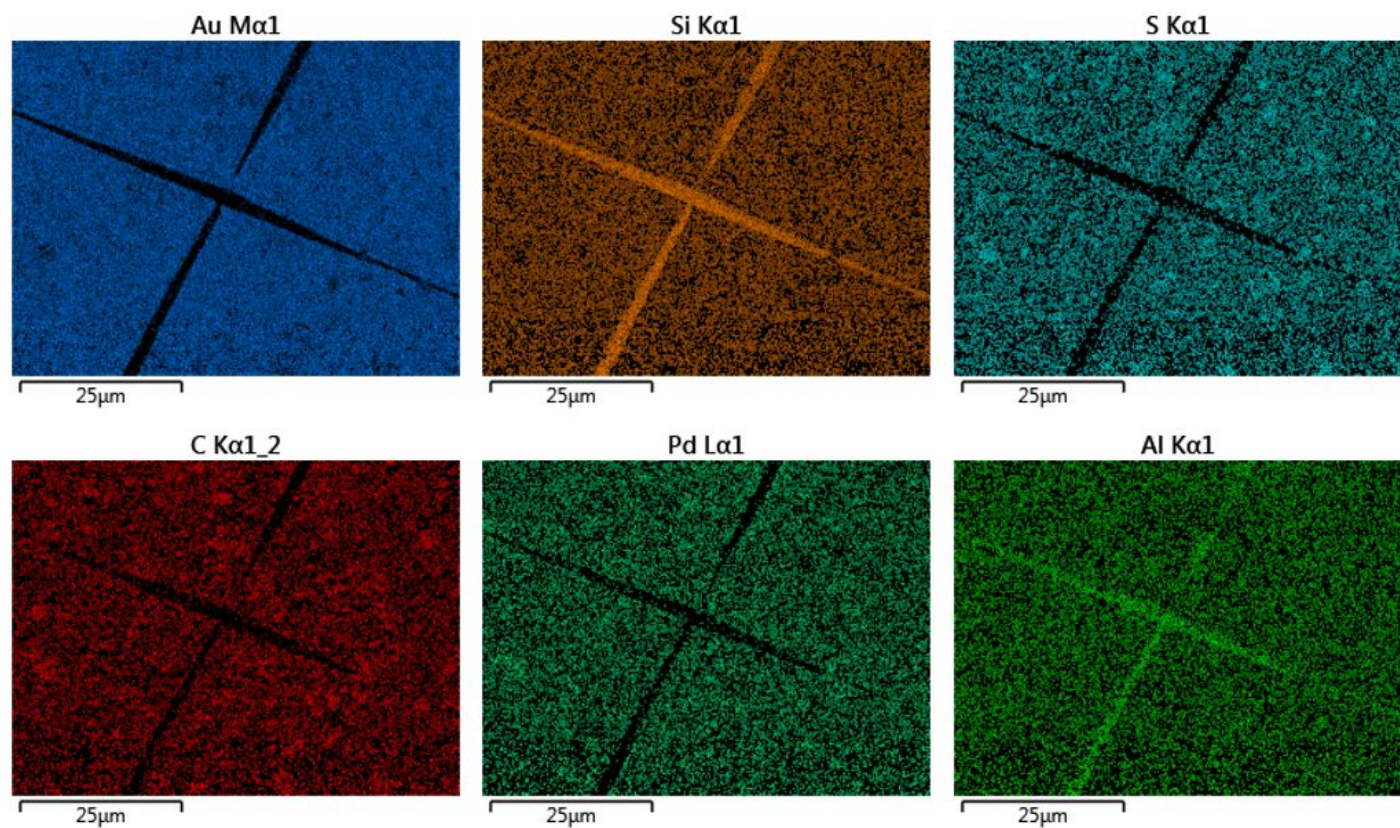


**Figure S1.** EDS element mapping of the cracked gold film substrate in Fig. 7b. The carbon and sulfur signals are strongly associated with the surface of the film and are negligible in the crack, consistent with a layer of polythiophene grown on the upper surface of the gold film.

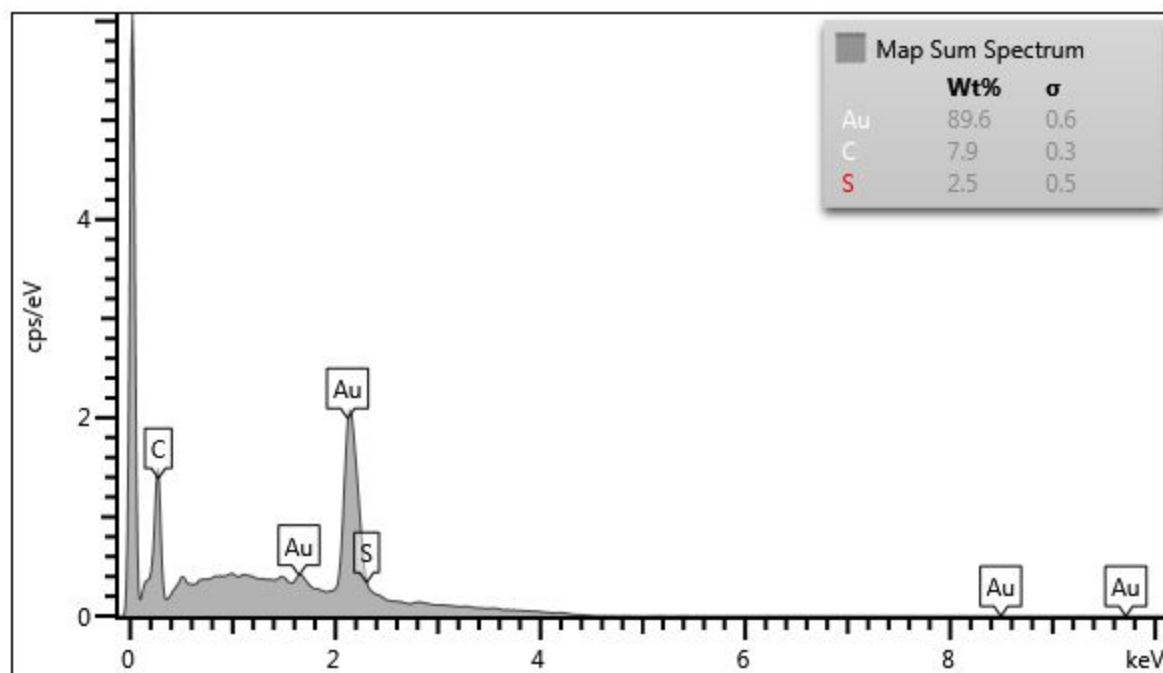
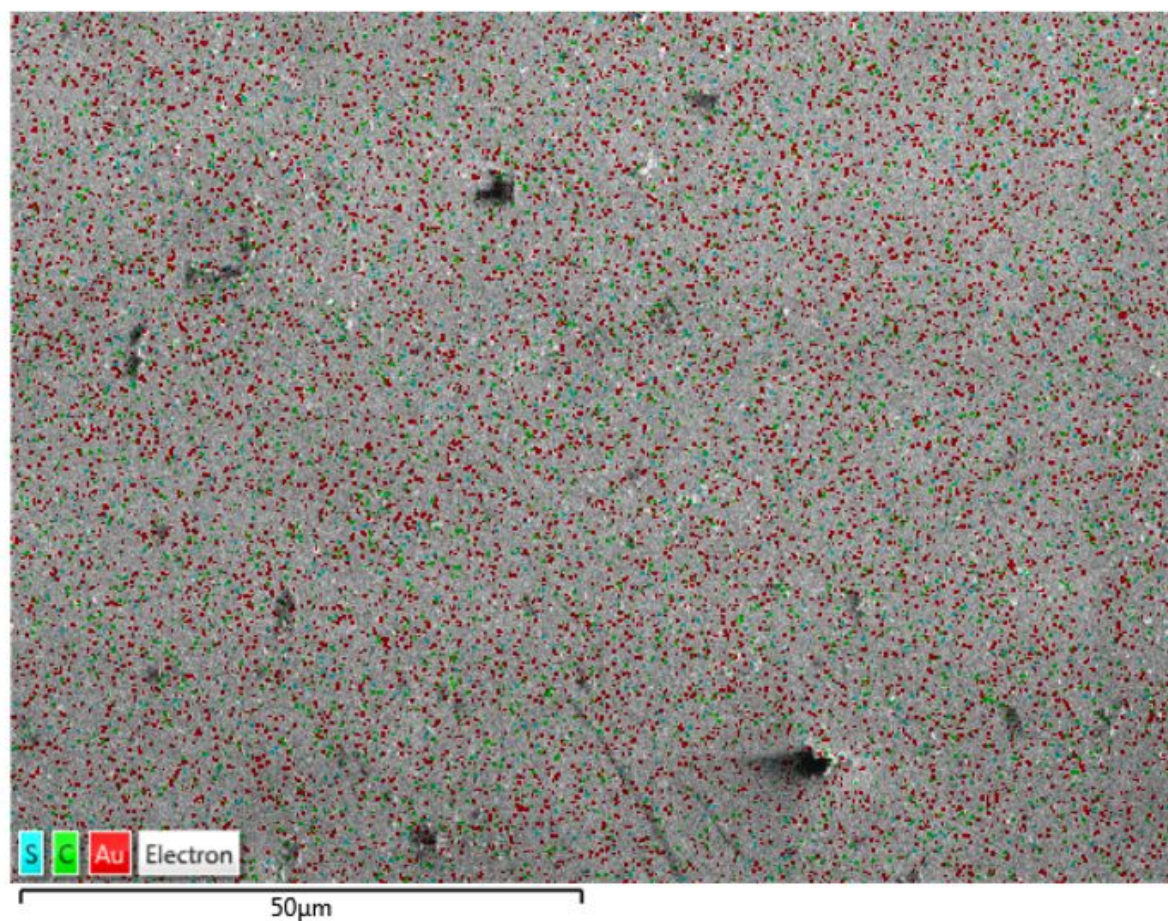


**Figure S2.** EDS element mapping and spectrum of the cleaned substrate in Fig. 7c.



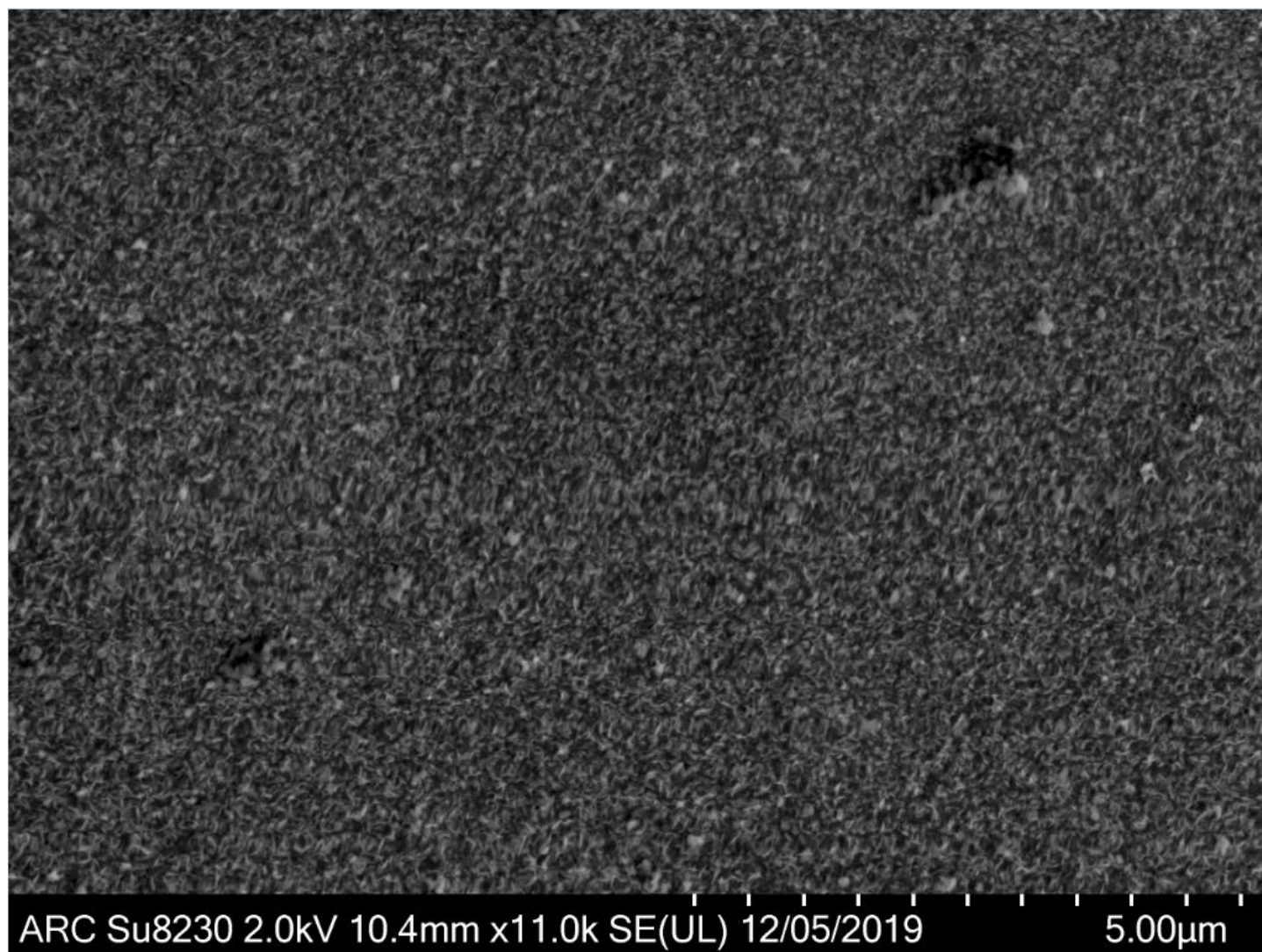


**Figure S3.** SEM micrograph of the PT film produced by the PEPPSI catalyst.

\*“ $t$  h/  $n$  eq.” denotes that 50 mM  $\text{FcCH}_2\text{ThBr}$  was reacted with  $n$  equiv. of  $i\text{-PrMgCl}\cdot\text{LiCl}$  solution for  $t$  time at  $0^\circ\text{C}$  under nitrogen.

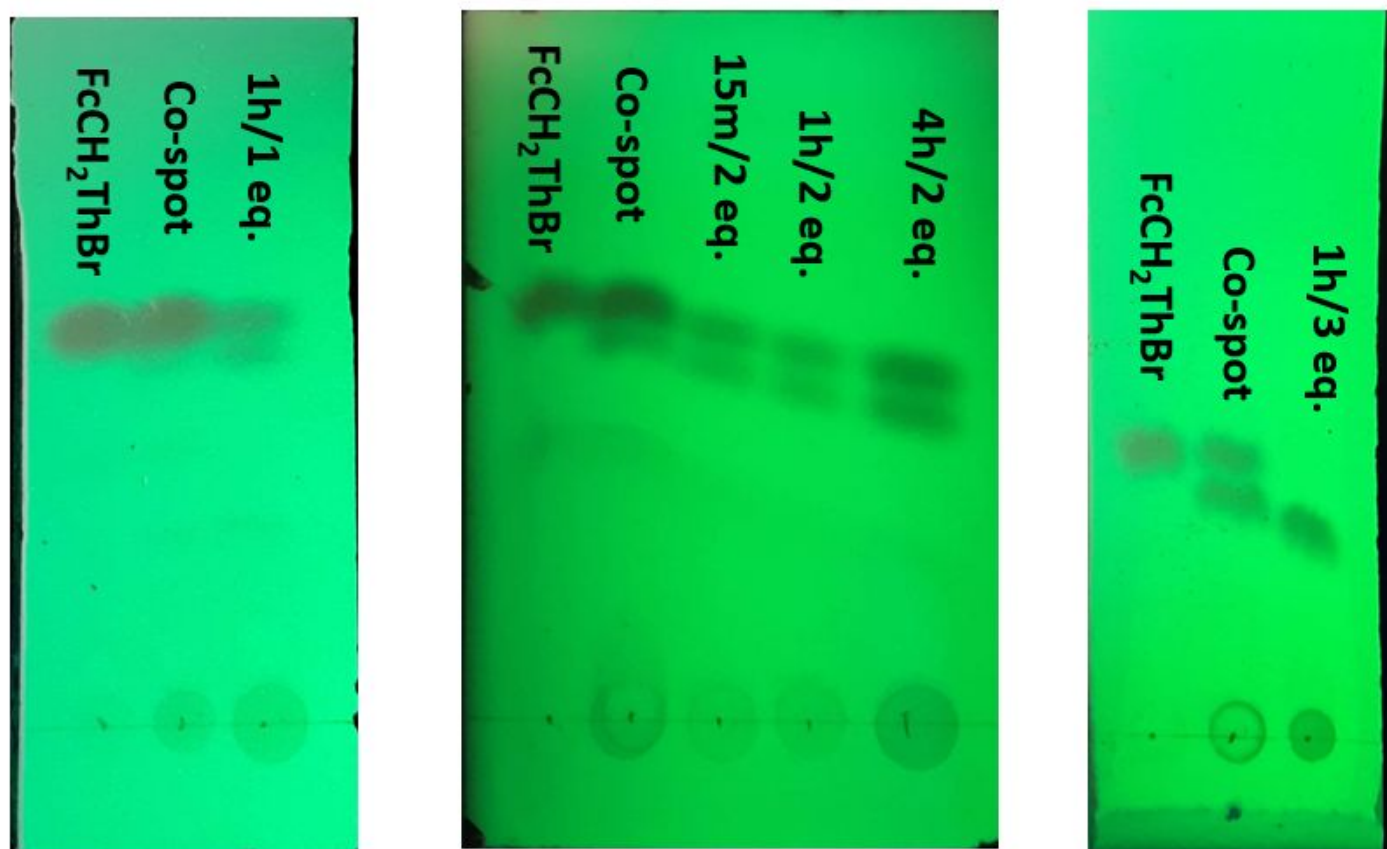


**Figure S4.** TLC (hexanes) of water-quenched aliquots of the magnesiated ferrocene probe  $\text{FcCH}_2\text{ThMgCl}$  as prepared by magnesium/halogen exchange under various conditions. Reactions were performed in dry THF solvent using freshly titrated commercial  $i\text{-PrMgCl}\cdot\text{LiCl}$  2-methylTHF solution, in a Schlenk flask under ultrapure nitrogen from a Schlenk line, while cooling in a water/ice bath. TLC indicates only partial conversion of  $\text{FcCH}_2\text{ThBr}$  to  $\text{FcCH}_2\text{ThMgCl}$  between 1 and 2 equivalents of  $i\text{-PrMgCl}\cdot\text{LiCl}$  solution.

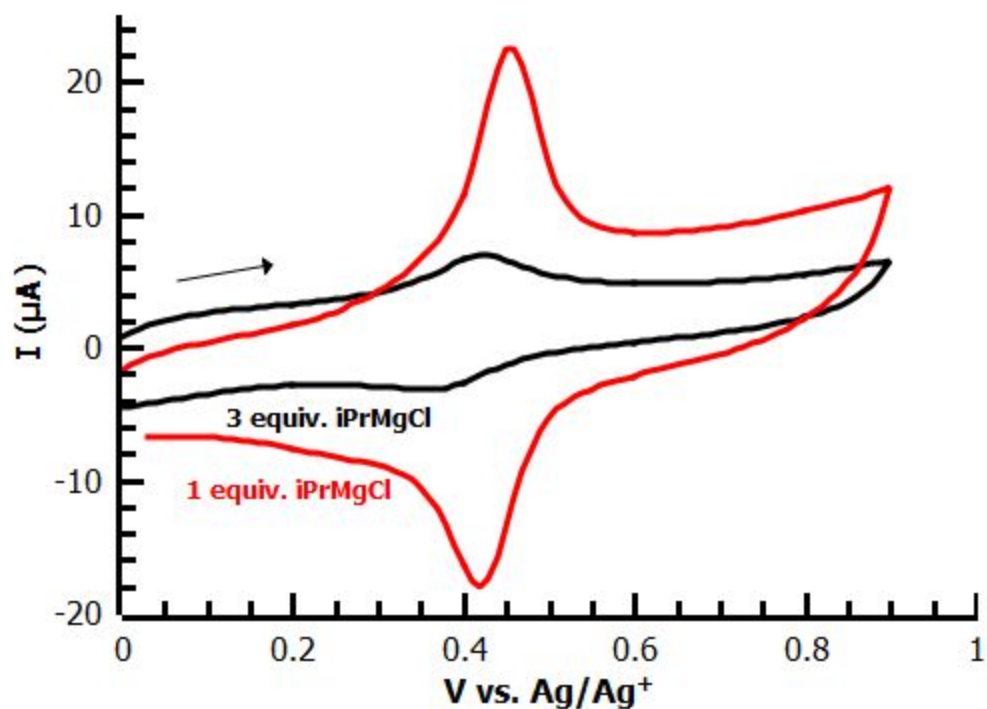


**Figure S5.** Cyclic voltammetry of aryl iodide-functionalized substrates coupled with ferrocene probe  $\text{FcCH}_2\text{ThMgCl}$  prepared under various conditions. Despite lower conversion, use of an excess of  $\text{FcCH}_2\text{ThBr}$  yields much higher surface coverage of ferrocenyl groups than an excess of  $\text{iPrMgCl}$ . Curves correspond to coupling solutions "1h/1eq" (red) and "1h/3eq" (black), respectively, in Figure S4.



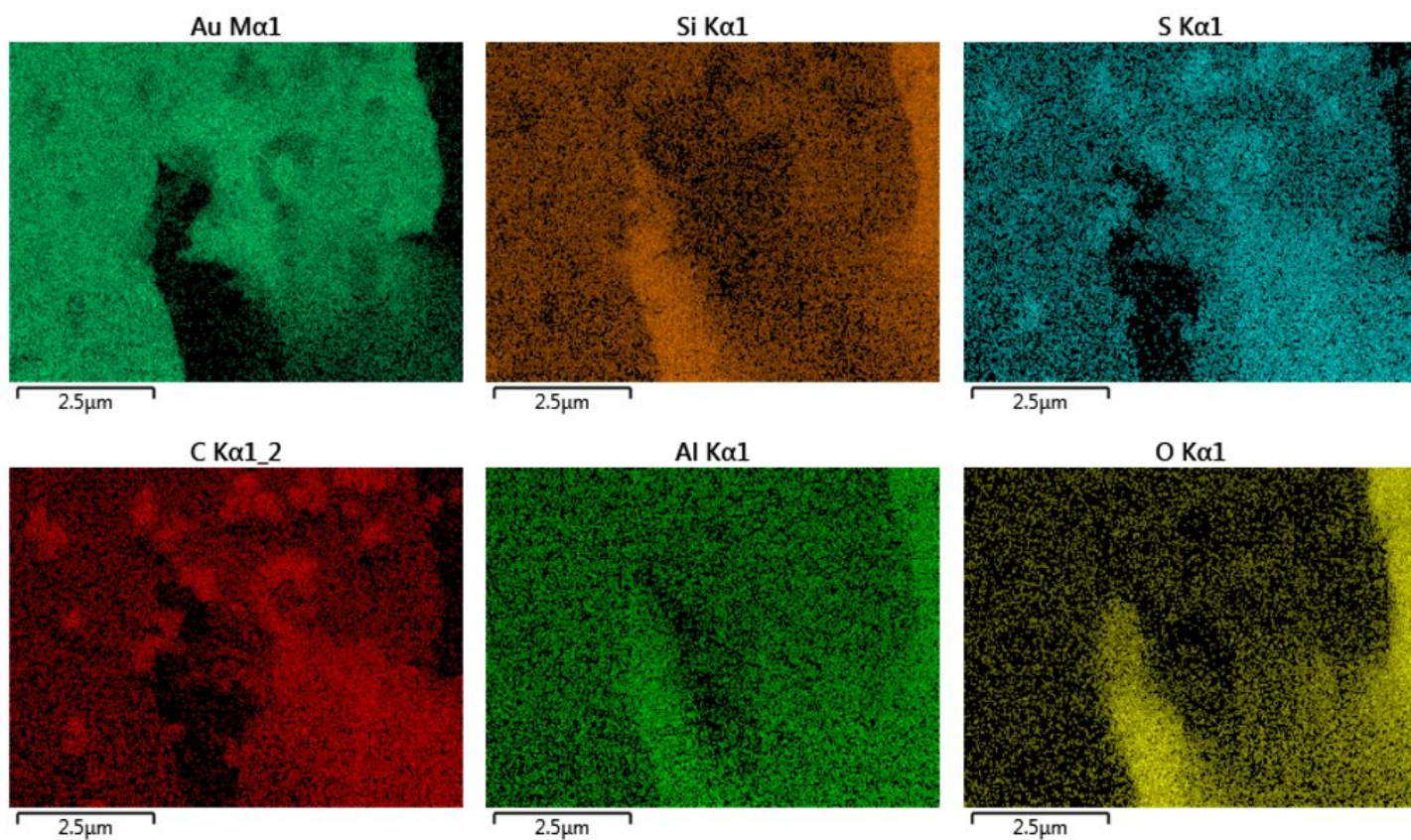
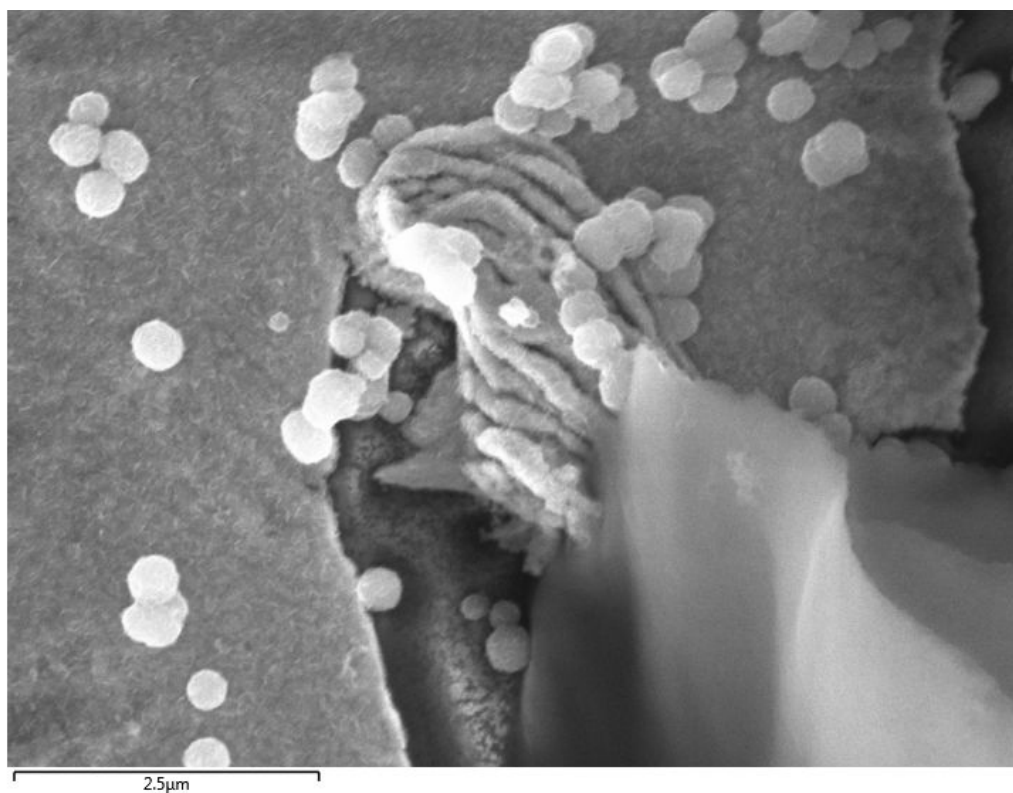


**Figure S6.** EDS elemental mapping of a damaged region in the film before rigorous cleaning confirms that the rough surface below PT nanoparticles is also PT, with S and C signals associated with both the surface and nanoparticles.

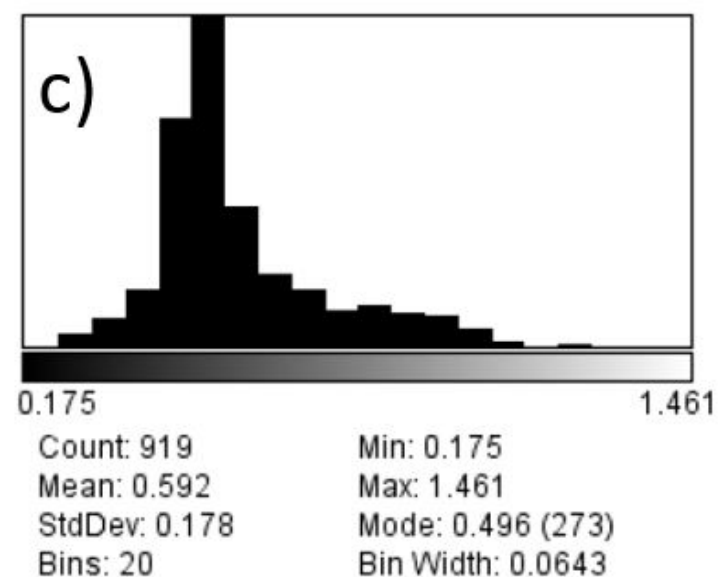
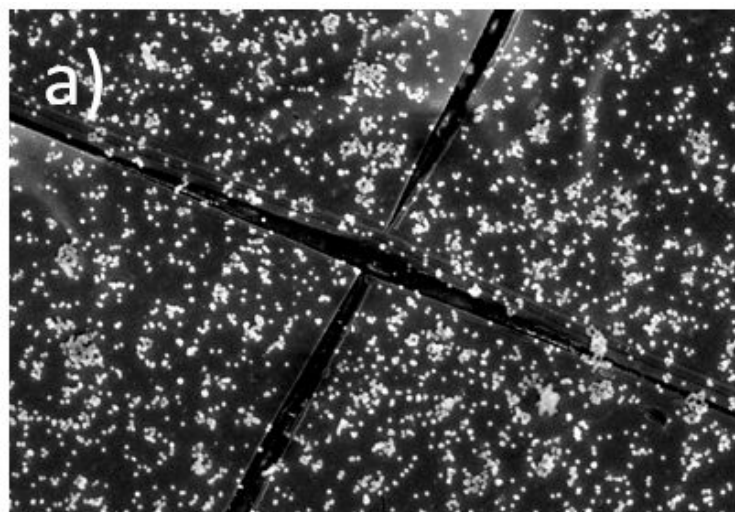


**Figure S7.** The raw image (a) from Fig. 6(b) was processed in ImageJ to identify isolated particles (b). The distribution of Feret diameter (caliper diameter) of isolated particles, (c), shows a mean of 592 nm and narrow band near 500 nm, the diameter of the typical particle found. An artifact band near 1000 nm is due to occasional dimer aggregates registering as a 1  $\mu$ m particle.



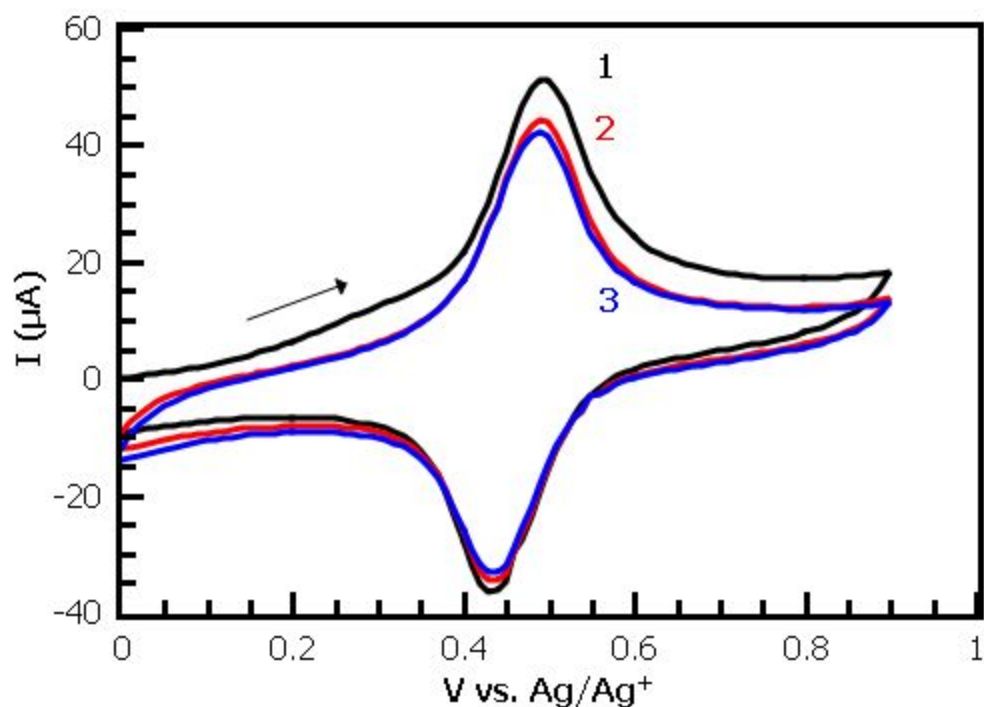


**Figure S8.** A typical CV measurement of a freshly coupled initiator film ( $\text{FcCH}_2\text{ThMgCl}$  with PhI initiator) showing three CV cycles. Integrated current generally declines sharply after the first cycle, and steadily (ca. 2%/cycle) after that. All calculated surface coverages, because of the observed decline, are based on the second cycle.

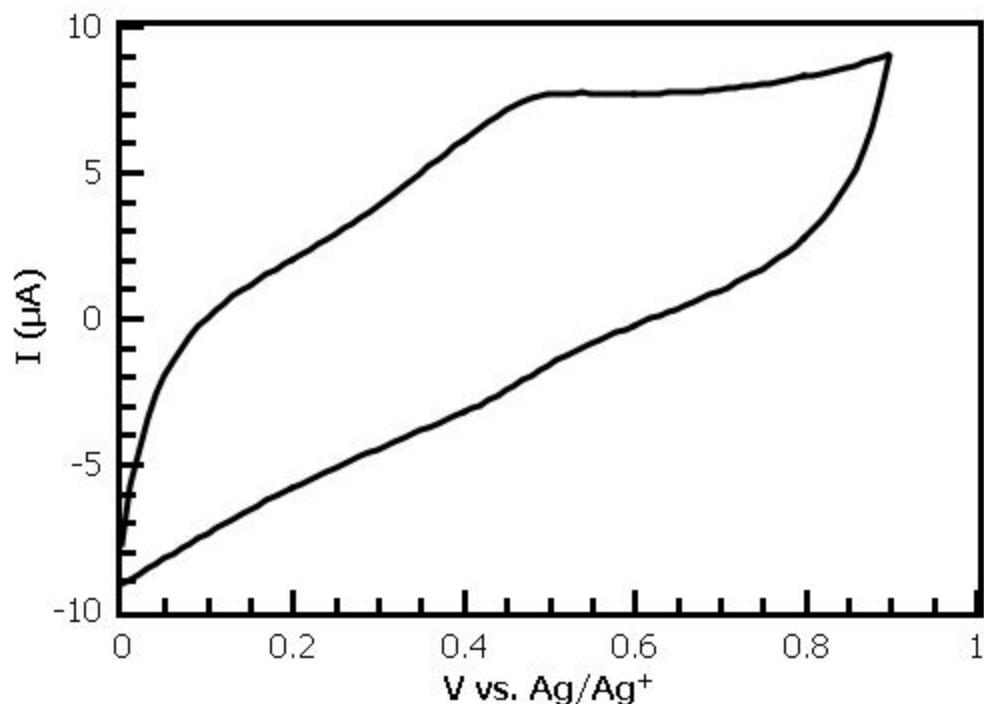


**Figure S9.** CV measurement of a 4-bromobenzenediazonium-derived initiator (deposited under the same conditions as 4-iodobenzenediazonium, Figure S7, gives a nonideal redox couple with a

surface coverage (calculated only from the oxidation peak) of  $6.1 \times 10^{-12}$  mol/cm<sup>2</sup>, roughly 13% of the surface coverage obtained from the iodine-based initiator.

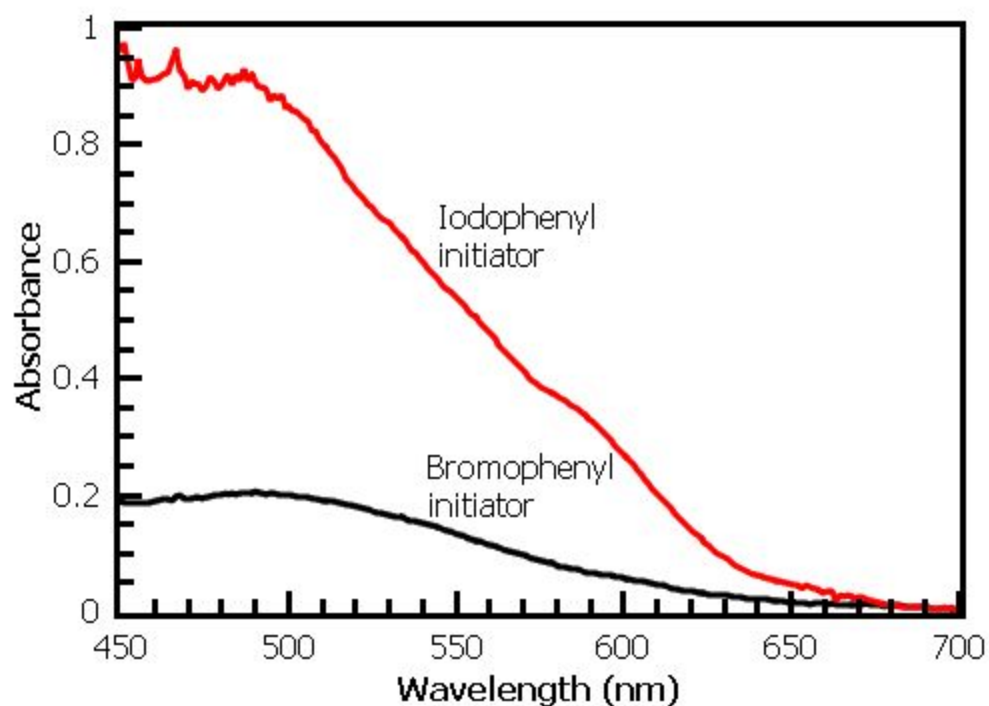


**Figure S10.** Reflectance UV-visible light spectroscopy of PT films polymerized under identical conditions using iodophenyl (Figure S7) and bromophenyl (Figure S8) initiators. Under these conditions, not optimized for the use of the bromophenyl coupling agent, the coverage of both ferrocene probe and surface polythiophene is much lower.

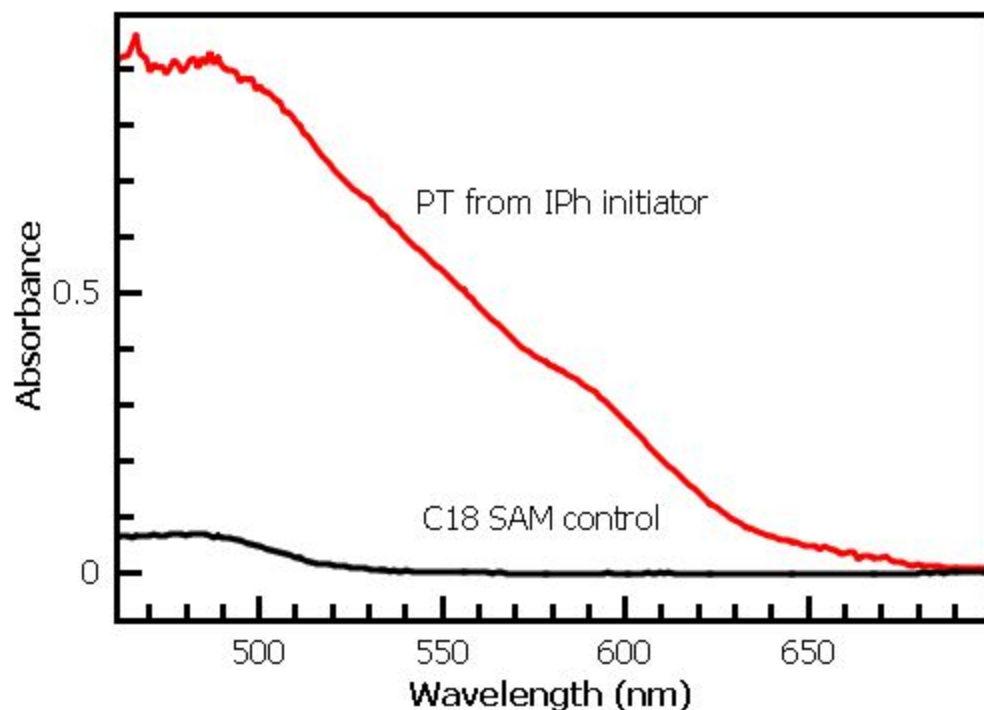


**Figure S11.** Reflectance UV-visible light spectroscopy of a plain C18 thiol SAM subjected to polymerization conditions from Fig. S9, with the IPh initiator film data shown for context. A small absorption, likely due to the physisorbed polymer seen in Figure 6 and S6, is visible.

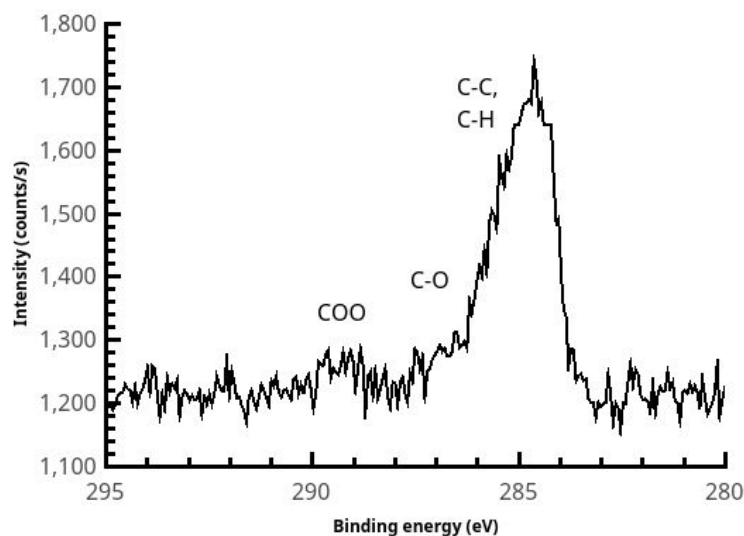


**Figure S12.** A new-from-the-manufacturer Au slide, thoroughly cleaned using "piranha" oxidizer, still shows features of adventitious carbon in XPS.

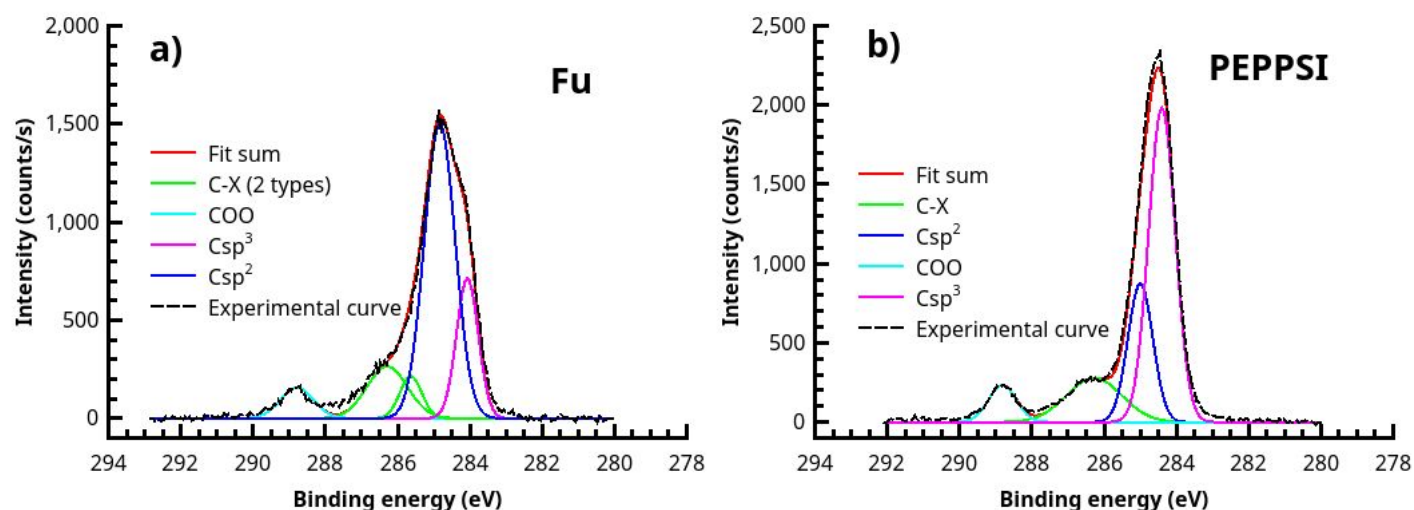


**Figure S13.** Detailed fitting of C1s XPS data from (a) PT-Fu and (b) PT-PEPPSI films shows a larger fraction of Csp<sup>2</sup> carbons, as well as noticeable oxidation peaks from air doping of the electron-rich polymer.



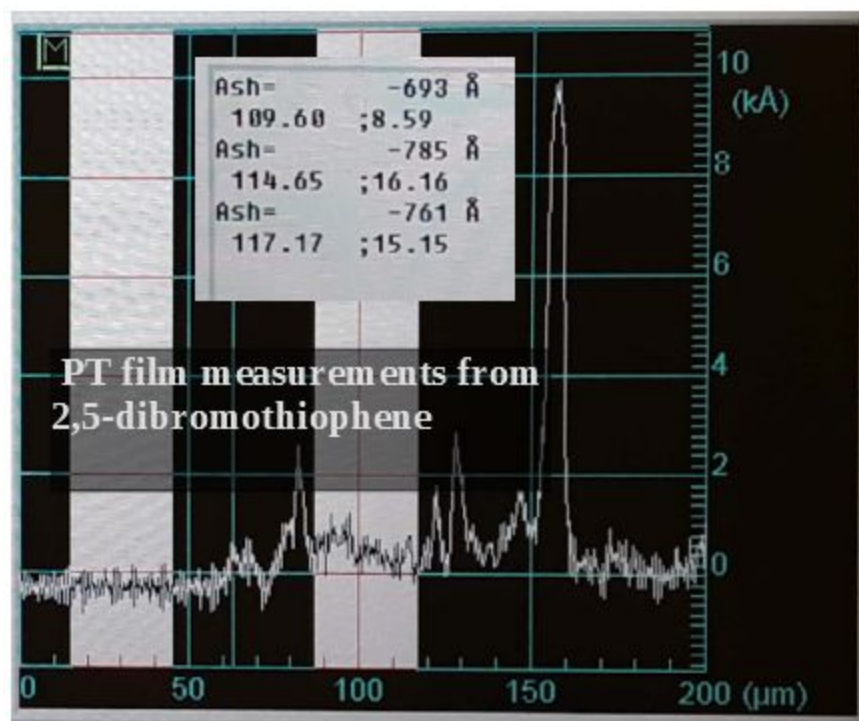
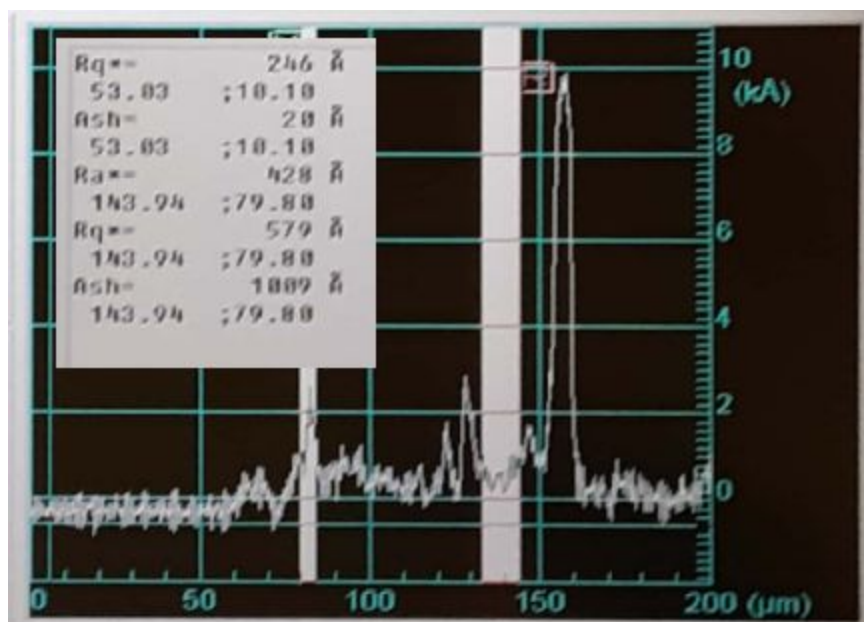


**Figure S14.** Screen-captured profilometry of the PT-Fu film reveals the surface roughness of 40-50 nm, the 70-80 nm average film thickness, and the presence of occasional very thick features and film edges.

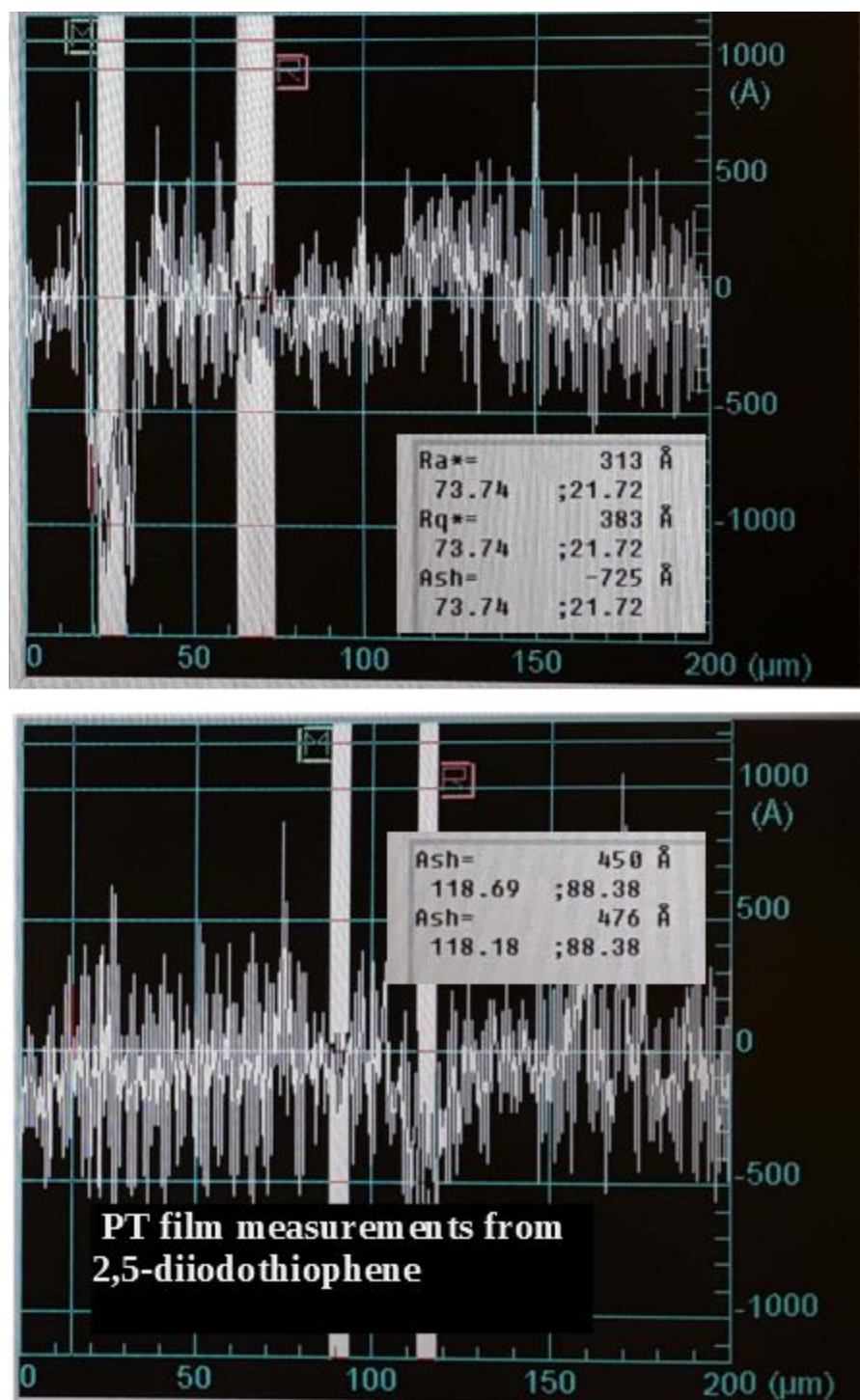


**Figure S15.** Screen-captured profilometry of the film produced from Fu catalyst with a diiodothiophene monomer shows a similar thickness to the bromothiophene monomer, but a detectably smoother (lower Ra) polymer film as well as fewer abnormally large features.

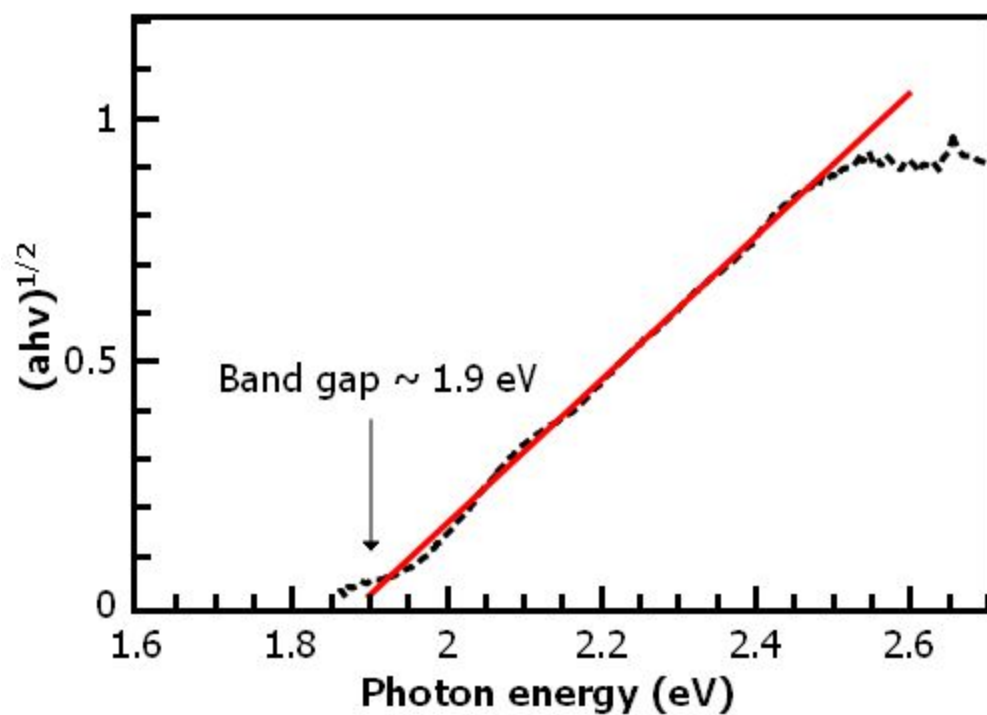


**Figure S16.** A Tauc plot derived from Fig. S10 can be extrapolated to a band gap of 1.9 eV, a reasonable value for polythiophene.

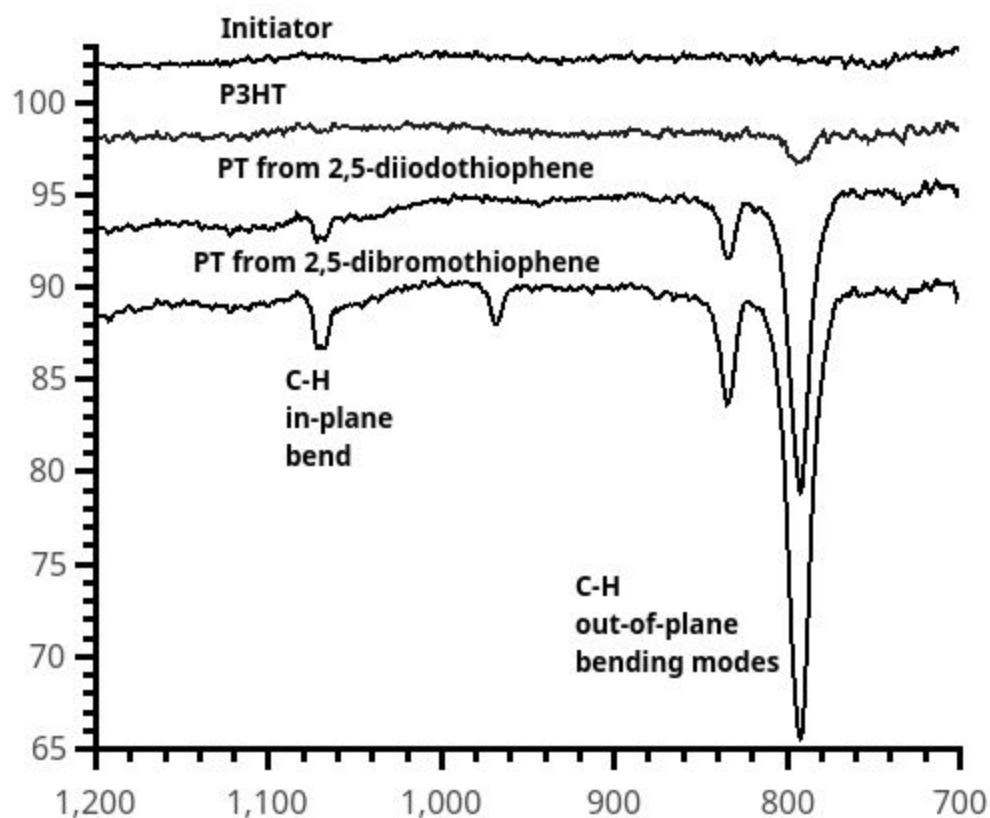




**Figure S17.** IR spectroscopy of films formed by polymerization of diiodothiophene and 2,5-dibromo-3-hexylthiophene are consistent with a thick film of PT formed by the iodo-based monomer, but a very thin film of P3HT due to rapid termination of the polymerization. The out-of-plane bend of the polymer can still be observed in the P3HT film.